

# Excitation of $^{208}\text{Pb}$ in light ion induced reactions and the two octupole phonon multiplet

B. D. Valnion,<sup>1,2</sup> V. Yu. Ponomarev,<sup>1,3</sup> Y. Eisermann,<sup>1</sup> A. Gollwitzer,<sup>1</sup> R. Hertzenberger,<sup>1</sup> A. Metz,<sup>1</sup> P. Schiemenz,<sup>1</sup> and G. Graw<sup>1</sup>

<sup>1</sup>*Sektion Physik der Universität München, D-85748 Garching, Germany*

<sup>2</sup>*Göller Verlag GmbH, Aschmattstr. 8, D-76532 Baden-Baden, Germany*

<sup>3</sup>*Bogoliubov Laboratory of Theoretical Physics, JINR, RU-141980 Dubna, Russia*

(Received 4 July 2000; published 23 January 2001)

To identify the states of the  $0^+$ ,  $2^+$ ,  $4^+$ , and  $6^+$  two octupole phonon (TOP) multiplet in  $^{208}\text{Pb}$  and their respective fragmentation inelastic proton, deuteron, and  $\alpha$  scattering has been measured in high energy resolution. Quantum numbers and spectroscopic factors of excited states up to 8 MeV are obtained from the  $^{207}\text{Pb}(d,p)^{208}\text{Pb}$  transfer reaction with vector polarized deuterons. From the comparison with literature, we conclude that up to  $E_x=6$  MeV, essentially all states are resolved. The data are compared with recent calculations within the quasiparticle phonon model. For the lowest states the calculated energies are in excellent agreement with experiment. The calculated spectrum of  $0^+$ ,  $2^+$ ,  $4^+$ , and  $6^+$  states, which includes mixing with the TOP multiplet, is related to experimental states up to excitation energies above twice the excitation energy of the collective  $3_1^-$  state at  $E_x=5230$  keV. The measured excitation strengths are consistent with the predicted fragmentation of the two octupole phonon states.

DOI: 10.1103/PhysRevC.63.024318

PACS number(s): 27.80.+w, 21.10.Jx, 21.60.-n, 25.45.-z

## I. INTRODUCTION

Because of double shell closure, the experimental resolution of the excitation spectrum of  $^{208}\text{Pb}$  remains a subject of considerable efforts. Recent  $(d,p\gamma)$  [1–3],  $(n,n'\gamma\gamma)$  [4–7] studies, heavy ion induced gamma decay [8–12], inelastic light ion [13,14], and photon scattering experiments [15] provide complete spectroscopic information for excitation energies up to  $E_x=4.9$  MeV and identification of many states at excitation energies up to the neutron emission threshold and above. The main motivation of these studies has been to extend the upper limit of the complete spectroscopy in this nucleus and to study the properties of some specific states, namely two octupole phonon (TOP) states, which are still uncertain after a long time of investigation.

To achieve these goals inelastic scattering  $(p,p')$ ,  $(d,d')$ , and  $(\alpha,\alpha')$  experiments with a high resolution have been performed. The first two reactions are nonselective and allow to excite all levels which is suitable for our purpose. Quantum numbers of observed levels have been obtained from analysis of angular distributions. Inelastic  $\alpha$  scattering is a complimentary reaction; since only natural parity levels are excited, its results are used as additional evidence in nonuclear situations with quantum numbers assignment. In these studies, several levels in  $^{208}\text{Pb}$  unknown previously have been detected.

The information on excitation energies and quantum numbers of levels from inelastic scattering has been completed by spectroscopic factors measured in  $^{207}\text{Pb}(d,p)^{208}\text{Pb}$  transfer reaction with vector polarized deuterons. By this we investigate fragmentation of one-particle–one-hole (1p1h) configurations one has to expect near the Fermi surface, over low-lying excited states in this nucleus. In this energy range we have dominance of 1p1h excitations, most of them with negative parity because of double shell closure. The few positive parity states are those 1p1h excitations which include one of the  $\pi h_{11/2}$ ,  $\pi i_{13/2}$ ,  $\nu i_{13/2}$ , or the  $\nu j_{15/2}$  spin-

orbit intruders. The mixing of 1p1h excitations, the related prediction of collectivity, and the calculation of the excitation energies of the energetically lowest 2p2h dominated states are a point of theoretical relevance [16–20].

Concluding that essentially all levels below 6 MeV have been observed in the present studies, the properties of  $0^+$ ,  $2^+$ ,  $4^+$ , and  $6^+$  levels will be examined to assign the TOP states. The identification of the TOP states is essential to verify the vibrational nature of the lowest excited state in this nucleus, the  $3_1^-$  state at  $E_x=2614.5$  keV. In  $^{208}\text{Pb}$ , in the limit of ideal TOP collectivity, the  $0^+$ ,  $2^+$ ,  $4^+$ , and  $6^+$  multiplet is expected near 5229 keV at twice the excitation energy of the  $3_1^-$  state, which is the most collective state in  $^{208}\text{Pb}$  with a ground state transition probability of  $B(E3)=33$  single particle units [21] or a respective vibrational deformation parameter  $\beta_3=0.105$  as observed in  $(d,d')$  reaction [22]. Although several different experiments have been performed for this purpose [4–7,9–15], only the  $0^+$  member of this multiplet has been identified by two consequent  $E3$  decays [6].

The results of the present experimental studies will be compared with quasiparticle phonon model (QPM) [23] calculations. This model employs a large single-particle basis to construct phonon excitations of nuclei. Thus no additional effective charges are needed to reproduce the collectivity of the lowest vibrational states. An asset of this model is the possibility to describe low-lying states below threshold by wave functions which include a practically complete basis of one-, two-, and three-phonon configurations. The matrix elements of interaction between these configurations are calculated on a microscopic footing making use the internal fermion structure of the phonons. The internal fermion structure of phonons is also taken into account to exclude spurious  $n\bar{p}n\bar{h}$  components which violate Pauli principle in the wave functions of multiphonon configurations. The projection of  $n\bar{p}n\bar{h}$  configurations into the space of  $n$ -phonon configura-

tions and keeping the fermion structure of the latter in all analytical stages of this approach, makes it very easy to select (truncate) essential (nonessential) configurations depending on the properties of the states under consideration if computation problems arise due to the large configuration space involved.

Calculations in  $^{208}\text{Pb}$  have been performed self-consistently with the ones in neighboring  $A=207$  and  $209$  odd nuclei. This procedure allows to extract the information on the single particle basis from experimental data with good accuracy. Excited states with spin and parity from  $0^\pm$  to  $7^\pm$  and  $8^+$  are considered.

## II. EXPERIMENTS AND DATA ANALYSIS

Because of the spin of the projectiles, proton and deuteron scattering are nonselective reactions. The present experiments with these projectiles have been performed with line width down to 4 keV FWHM and essentially all states have been resolved. In contrast to this  $\alpha$  scattering is restricted to the excitation of states with natural parity. The  $^{207}\text{Pb}(d,p)$  transfer as a one-step process proceeds via the  $\nu(l_j \otimes p_{1/2}^{-1}; J^\pi)$  configuration in the wave function of the excited state with spin and parity  $J^\pi$ . Significant transfer probabilities is expected for the neutron orbitals above the  $N=126$  shell closure; these are the  $4s_{1/2}$ ,  $3d_{3/2}$ ,  $3d_{5/2}$ ,  $2g_{7/2}$ ,  $2g_{9/2}$ ,  $1i_{11/2}$ , and  $1j_{15/2}$  orbitals, hence  $(d,p)$  is restricted to the excitation of  $(0-6)^-$  and  $(7-8)^+$  states. Thus the  $0^+$ ,  $2^+$ ,  $4^+$ , and  $6^+$  states have to show up in all of these scattering reactions, but not in  $(d,p)$  transfer.

The experiments use the Q3D magnetic spectrograph [24] at the Munich MP tandem accelerator and a multilayer focal plane detector [25], which is a combination of position sensitive proportional wire energy loss detectors (with additional cathode read out) and a rest energy scintillation detector. This arrangement provides focal plane reconstruction and particle identification [26].

### A. Inelastic scattering

Inelastic proton scattering has been measured at 22 MeV incident beam energy (200 nA beam intensity) at a scattering angle of  $\theta=50^\circ$  with full Q3D acceptance of  $\Delta\Omega=10.8$  msr for excitation energies up to 7000 keV. Because of a self-supporting target of  $239 \mu\text{g}/\text{cm}^2$  and 99.86% enriched  $^{208}\text{Pb}$ , impurity lines are negligible.

For each magnetic spectrograph setting the line width was in between 4 and 5 keV FWHM over a range of about 2 MeV of excitation energy (corresponding to a range of 1.0 m along the 1.7 m focal plane). The spectra had been fitted using a modified search program GASPAN [27,28], with some restriction about the line shape, which is kept constant within some appropriate intervals of excitation, being the only input.

In the upper part of Fig. 1 the proton scattering spectrum and a respective fit is shown for a 450 keV interval around twice the excitation energy of the  $3_1^-$  state at  $E_x=5229$  keV. (A complete presentation of the experimental data is given in the thesis of B. D. Valnion [27].)

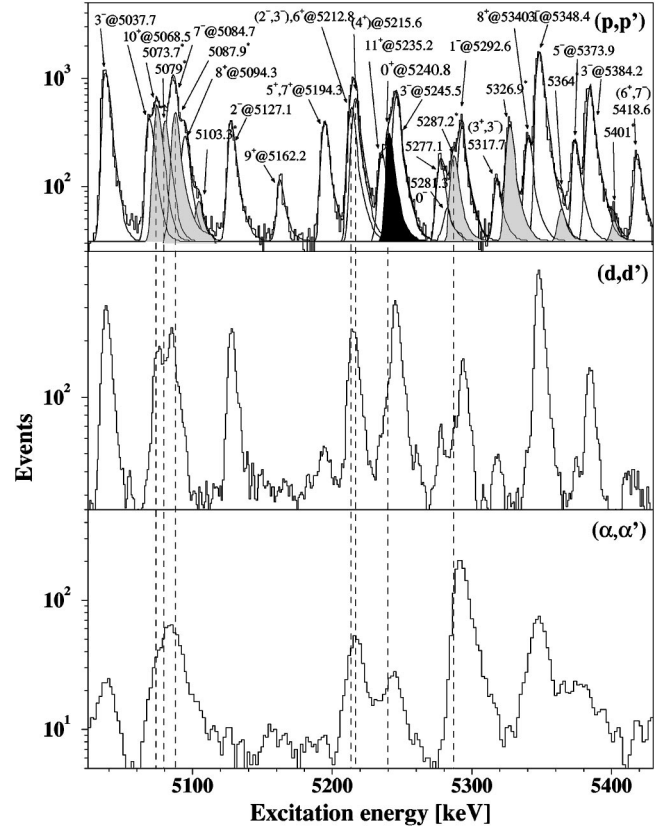


FIG. 1. Part of the scattering spectra for  $(p,p')$  and  $(d,d')$  at  $\theta_{\text{lab}}=50^\circ$  (top and middle) and  $(\alpha,\alpha')$  at  $\theta_{\text{lab}}=25^\circ$  as function of the excitation energy (see text for details).

The asymmetry of the shape is due to Landau scattering. The observed line widths mainly originate from fluctuations of the beam energy and from ion optical features of the whole assembly; thus a relatively thick target could be used.

Excitation energies are obtained from the line positions using polynomials, adjusted to reproduce a number of known states. These energies and the scattering cross sections are listed in Table I for the range up to 6100 keV (for higher excitation energies, see Ref. [27]) and compared with the most recent values from  $\gamma$  spectroscopy, as summarized by Schramm *et al.* [1].

For isolated peaks of good statistics the energy determination agrees within 1 keV or better; deviations in this range are expected because of nonlinearities in the cathode read out of the detector. For weak and strongly overlapping peaks, as in the range shown in Fig. 1, the excitation energies deviate up to 1.5 keV. In Table I, these  $(p,p')$  energies are compared with literature values, a unique relation of the latter ones to the states observed is obvious.

In Fig. 1 the known states are indicated with their  $J^\pi$  values and excitation energies. The states observed for the first time, five of them with considerable cross section, are shaded. The known 5075.8 keV state (without  $J^\pi$  assignment in the literature) is near to the known  $10^+$  level at 5069.4 keV,  $7^-$  level at 5085.5 keV, and  $8^+$  level at 5093.1 keV. The fit, reproducing these assigned levels, introduces instead of the 5075.8 keV state two states at 5074 keV and 5079

TABLE I. States in  $^{208}\text{Pb}$ : the excitation energies are from  $(p,p')$ , as information about the excitation strengths the cross sections for  $(p,p')$ ,  $(\alpha,\alpha')$ , and  $(d,p)$  are listed. Spectroscopic factors are given if determined. For comparison with the literature we refer to the numbering, excitation energies, and quantum numbers, as given in the recent compilation of Schramm *et al.* [1].

No.	According to Schramm <i>et al.</i>		This work				$G_{ij}$
	$E_x$ [keV]	$J^\pi$ [ $\hbar$ ]	$(p,p')$		$(\alpha,\alpha')$	$(\vec{d},p)$	
			$E_x$ [keV]	$\sigma(50.0^\circ)$ [ $\mu\text{b/sr}$ ]	$\sigma(27.5^\circ)$ [ $\mu\text{b/sr}$ ]	$\sigma(25.0^\circ)$ [ $\mu\text{b/sr}$ ]	
1	0.000	$0^+$					
2	2614.549(13)	$3^-$	2614.5(3)	1000	7500	$\sim 20$	
3	3197.740(13)	$5^-$	3197.7(3)	440	700	400	
4	3475.103(15)	$4^-$	3475.1(14)	42		460	
5	3708.511(43)	$5^-$	3708.5(3)	780	$< 20$	105	
6	3919.987(70)	$6^-$	3920.0(3)	125			
7	3946.620(100)	$4^-$	3946.6(3)	4			
8	3961.138(46)	$5^-$	3961.1(3)	35	42		
9	3995.585(60)	$4^-$	3995.6(3)	35		$< 20$	
10	4037.514(75)	$7^-$	4037.5(3)	68	148		
11	4051.194(40)	$3^-$	4051.2(3)	22	$< 20$	$< 20$	
12	4085.450(150)	$2^+$	4085.4(3)	270	848		
13	4125.444(44)	$5^-$	4125.4(5)	15	37	88	$2g_{9/2}:0.135$
14	4180.200(100)	$5^-$	4180.2(5)	23	$< 20$	84	$1i_{11/2}:3.020$
15	4206.200(90)	$6^-$	4206.2(5)	12		185	$1i_{11/2}:6.360$
16	4229.620(50)	$2^-$	4229.6(5)	30		110	$3d_{5/2}:0.123$
17	4254.880(50)	$3^-$	4254.9(5)	22	36	20	$3d_{5/2}:0.032$
18	4262.000(55)	$4^-$	4262.0(5)	8			$2g_{9/2}:0.020$
19	4296.700(80)	$5^-$	4296.7(5)	9	30	30	$1i_{11/2}:0.930$
20	4323.930(130)	$4^+$	4323.9(5)	195	255		
21	4358.785(63)	$4^-$	4358.8(5)	24		68	$2g_{9/2}:0.105$
22	4383.246(65)	$6^-$	4383.2(5)	12		$< 10$	$1i_{11/2}:0.260$
23	4423.630(75)	$6^+$	4423.6(5)	130	268	$< 10$	
24	4480.750(100)	$6^-$	4480.7(5)	26	$< 20$	$< 10$	
25	4610.795(70)	$8^+$	4609.3(7)	26	144	89	$1j_{15/2}:5.295$
26	4680.310(250)	$(7^-)$	4680.7(5)	8	$< 20$		
27	4698.375(40)	$3^-$	4698.4(5)	57	242	860	$3d_{5/2}:0.965$
28	4709.409(250)	$5^-$	4709.5(35)	5	$\sim 30$	$\sim 30$	
29	4711.300(750)	$(4^-)$					
30	4761.800(250)	$(6^-)$	4761.8(5)	8		$< 10$	
30 (a)	see Ref. [21]	$(8,9,10)$	4833(2)	4			
31	4841.400(100)	$1^-$	4841.7(3)	52	224	$\sim 30$	
31 (a)	see Ref. [21]		4853(2)	3			
32	4857.500(350)						
33	4860.840(80)	$8^+$	4859.8(15)	8	$\sim 20$	50	$1j_{15/2}:2.650$
34	4866.840(80)	$0^+$	4866.9(15)	12	$< 20$		
35	4867.816(80)	$7^+$	see No. 34			138	$1j_{15/2}:7.500$
36	4895.277(80)	$10^+$	4894.8(15)	12	$< 20$		
36 (a)			4910.6(15)	5		$< 10$	$1j_{15/2}:0.440$
36 (b)	see Ref. [21]	$\geq 6$	4917.6(15)	12			
36 (c)	see Ref. [21]	$2^+$	4928.1(15)	8	$< 20$		
37	4937.550(200)	$3^-$	4937.1(3)	16	25	43	$3d_{5/2}:0.032$ $2g_{7/2}:0.025$
38	4953.320(230)	$3^-$	4952.2(3)	6	$< 20$	$< 10$	
38 (a)			4962.9(15)	6			

TABLE I. (*Continued*).

No.	According to Schramm <i>et al.</i>		This work				$G_{ij}$
	$E_x$ [keV]	$J^\pi$ [ $\hbar$ ]	$(p,p')$ $E_x$ [keV]	$\sigma(50.0^\circ)$ [ $\mu\text{b/sr}$ ]	$(\alpha,\alpha')$ $\sigma(27.5^\circ)$ [ $\mu\text{b/sr}$ ]	$(\vec{d},p)$ $\sigma(25.0^\circ)$ [ $\mu\text{b/sr}$ ]	
39	4974.037(40)	$3^-$	4974.2(6)	35	156	1750	$3d_{5/2}:1.683$
39 (a)	see Ref. [21]		4994.7(6)	6		20	$3d_{5/2}:0.020$
40	5010.550(90)	$9^+$	5010.0(6)	5			
41	5037.520(50)	$2^-(3^-)$	5037.2(6)	41	34	1500	$3d_{5/2}:1.470$
42	5069.380(130)	$10^+$	5068.5(15)	9	<20		
43	5075.800(200)		5073.7(15)	19	48	20	
44	5085.550(250)	$7^-$	5084.7(15)	26	50		
44 (a)			5087.9(15)	14	<20		
45	5093.110(200)	$8^+$	5094.3(15)	9	<20	$\sim 15$	
45 (a)			5103.3(15)	1			
46	5127.420(90)	$2^-(3^-)$	5127.1(6)	14		881	$3d_{5/2}:0.836$
47	5134.720(450)						
48	5162.100(90)	$9^+$	5162.2(6)	3			
49	5193.400(150)	$5^+$					
50	5195.340(140)	$7^+$	5194.3(6)	14		25	$2g_{7/2}:0.038$
51	5213.000(200)	$6^+$	5212.8(15)	10		see No. 52	
51 (a)	see Ref. [21]	$(2,3)^-$	5213.3(4)			50	$3d_{5/2}:0.050$
52	5216.540(300)	$4^+$	5215.6(15)	21	61		
53	5235.440(180)	$11^+$	5235.2(15)	6			
54	5241	$0^+$	5240.8(15)	10	<20		
55	5239.350(360)						
56	5245.280(60)	$3^-$	5244.6(10)	20	25	920	$3d_{5/2}:0.858$
57	5254.160(150)						
57 (a)	see Ref. [21]	$3^-$	5277.1(15)	5		$\sim 20$	
58	5280.322(80)	$0^-$	5281.3(15)	2		490	$4s_{1/2}:0.650$
58 (a)			5287.2(15)	6	<20		
59	5292.000(200)	$1^-$	5292.6(15)	13	244	1390	$4s_{1/2}:1.550$
60	5317.000(200)	$(3^+)$	5317.7(6)	4			
61	5317.300(600)		see No. 60				
61 (a)			5326.9(6)	13			
62	5339.460(160)	$8^+$	5340.1(15)	10	<20		
63	5347.150(250)	$3^-$	5348.4(6)	64	87	110	$3d_{5/2}:0.018$ $2g_{7/2}:0.214$
63 (a)			5364(3)	1	<20		
63 (b)	see Ref. [21]	$5^-$	5373.9(15)	9			
64	5380.650(800)		see No. 66				
65	5383.74(111)		see No. 66				
66	5384.780(100)	$2^-(3^-)$	5384.2(6)	31	<20	160	$3d_{5/2}:0.155$
66 (a)			5401(2)	1			
66 (b)	see Ref. [21]		5418.6(5)	7			
67	5482.10(100)	$5^-$	5482.4(5)	75	367	<10	
68	5490.320(150)	$6^-$	see No. 68(a)				
68 (a)			5492.2(5)	31	80	51	$2g_{7/2}:0.066$
68 (b)			5502(3)	2			
69	5512.100(300)	$1^-$	5511.9(15)	63	624		$3d_{3/2}:0.165$
70	5516.600(350)	$3^-$	5516.9(15)	50		27	$2g_{7/2}:0.044$

TABLE I. (Continued).

No.	According to Schramm <i>et al.</i>		This work				$G_{ij}$
	$E_x$ [keV]	$J^\pi$ [ $\hbar$ ]	$(p, p')$		$(\alpha, \alpha')$	$(\vec{d}, p)$	
			$E_x$ [keV]	$\sigma(50.0^\circ)$ [ $\mu\text{b/sr}$ ]	$\sigma(27.5^\circ)$ [ $\mu\text{b/sr}$ ]	$\sigma(25.0^\circ)$ [ $\mu\text{b/sr}$ ]	
70 (a)			5524(3)	3			
70 (b)			5529(3)	2		~30	
71	5536.640(200)	$10^+$	5536.9(15)	14			
72	5542.040(180)	$7^-$	5543.3(15)	27	45		
73	5545.470(110)	$5^-$	see No. 72				
74	5548.080(200)		5547.5(15)	26		69	$3d_{5/2}:0.063$ $3d_{3/2}:0.011$
74 (a)			5554(2)	2			
75	5563.580(140)	$(3^-, 4^-)$	5564.7(6)	50	235	180	$3d_{5/2}:0.139$
76	5566.000(600)		see No. 75				
76 (a)			5576.6(15)	1			
76 (b)			5587.7(5)	2		<10	
77	5599.400(80)	$0^-$	5599.6(4)	11		92	$4s_{1/2}:0.103$
77 (a)	see Ref. [21]	$\geq 6$	5615.4(4)	3			
78	5641.100(500)		5639.9(15)	5	27	40	
78 (a)			5643.1(15)	8		40	
79	5649.700(280)	$(5^-)$	5649.8(9)	1			
79 (a)	see Ref. [21]	$5^-$	5658.8(25)	21	25	~20	
79 (b)			5666.4(15)	2	35		
80	5675.170(270)	$(4^-)$	5675.3(4)	9		~20	
81	5686.860(600)	$6^-$	5686.2(15)	8		<10	
82	5689.950(300)	$4^+$	5690.2(15)	32	114		
83	5695.100(500)	$7^-$	5694.8(15)	14			
84	5715.900(900)	$(2^+)$	5715.2(15)	3			
84 (a)	see Ref. [21]	$(7^-)$	5721.8(4)	17	67	<10	
84 (b)	see Ref. [8]	$6^+$	5738.4(8)	8			
84 (c)	see Ref. [21]	$(9^-)$	5741.1(4)	2		<10	
85	5750	$11^+$	5749.7(4)	4			
85 (a)	see Ref. [21]	$6^+$	5763.7(8)	4			
86	5777.900(120)	$3^-$	5778.1(4)	8		285	$3d_{5/2}:0.033$ $3d_{3/2}:0.220$
87	5782.000(600)						
88	5799.300(500)		5799.9(8)	2			
89	5805.900(900)	1	5804.9(15)	14			
90	5813.210(170)	$3^-(4^-)$	5813.4(4)	88	306	243	$2g_{7/2}:0.400$
91	5826.190(500)	$(8^+)$	5823.9(15)	5		~20	
91 (a)			5836.0(8)	9	35		
92	5846.10(110)	$1^+$	5844.8(15)	14			
93	5873.560(140)	$3^-$	5873.4(4)	15	43	1360	$2g_{7/2}:1.990$
94	5885.240(200)		5884.8(4)	19	<20	131	$3d_{5/2}:0.070$ $2g_{7/2}:0.106$
94 (a)	see Ref. [21]	$(8^+)$	5900(3)	1			
94 (b)	see Ref. [21]	$10^+$	5919(2)	6			
95	5923.734(40)	$2^-$	5922.3(15)	3		1885	$3d_{3/2}:1.700$
96	5928.000(300)	$10^+$					
97	5947.460(450)	$1^-$	5945.3(6)	13		1510	$3d_{3/2}:1.390$
98	5966.360(230)						
99	5968.600(60)	$4^-$	5967.8(8)	32		2890	$2g_{7/2}:4.580$
100	5972.870(370)	$2^+$					

TABLE I. (*Continued*).

According to Schramm <i>et al.</i>			This work				$G_{ij}$
No.	$E_x$ [keV]	$J^\pi$ [ $\hbar$ ]	$(p, p')$		$(\alpha, \alpha')$	$(\vec{d}, p)$	
			$E_x$ [keV]	$\sigma(50.0^\circ)$ [ $\mu\text{b/sr}$ ]	$\sigma(27.5^\circ)$ [ $\mu\text{b/sr}$ ]	$\sigma(25.0^\circ)$ [ $\mu\text{b/sr}$ ]	
100 (a)			5988.7(15)	12		$\sim 30$	
101	5992.640(260)	$6^+$	5994.9(15)	87	115	$\sim 30$	
102	6009.630(90)	$3^-$	6009.6(6)	79	308	643	$2g_{7/2}:1.020$
102 (a)			6020.4(20)	3			
103	6026.050(600)		6025.1(20)	3		$\sim 20$	
103 (a)			6033(2)	1			
103 (b)	see Ref. [21]		6037.8(15)	6		38	$(2h_{11/2}:0.045)$
103 (c)	see Ref. [21]	$4^+$	6053.7(6)	6	$< 20$		
103 (d)			6068.6(15)	1		$< 20$	$(2h_{11/2}:0.029)$
103 (e)			6077.7(15)	3		24	$(4s_{1/2}:0.038)$
104	6086.711(50)	$(2)^-$	6086.7(6)	15	32	605	$3d_{3/2}:0.570$
105	6099.850(370)		6098.9(15)	2			
106	6100.790(270)	$12^+$	see No. 105				
106 (a)			6101.9(15)	10		56	$(2h_{11/2}:0.075)$

keV. Because of the tight structure it remains open, whether one of these states is the 5075.8 keV state or not.

With respect to resolution, our data extend the information from a high resolution 35 MeV proton scattering experiment at MSU [29], where angular distributions have been also determined. In proton scattering, however, they are sensitive to microscopic features of the form factors and to additional contributions from exchange, which may modify significantly especially large angular momentum transfer excitations [30,31]. A detailed elaboration on this is beyond the scope of this study. The situation is less complicated for deuteron and  $\alpha$  induced scattering. Because of the absorption of the wave functions in the nuclear interior these reactions, especially the latter one, are sensitive to the asymptotic strength of the form factor. Therefore the vibrational collective model parametrization can be applied to calculate the angular distributions of the differential cross sections and to parametrize the excitation strengths of the experimental cross sections [30,32,33].

Angular distributions have been measured for inelastic deuteron scattering [27] at 22 MeV and for inelastic  $\alpha$  scattering [34] at 40 MeV, using 166 and 35  $\mu\text{g}/\text{cm}^2$  targets on 3 and 15  $\mu\text{g}/\text{cm}^2$  carbon backings, respectively. Part of the energy calibrated spectra of these reactions are shown in comparison with  $(p, p')$  in Fig. 1.

In a later deuteron scattering experiment an improved energy stabilization technique [35] was available; the respective energy resolution was down to 3.3 keV FWHM. [Because of technical reasons in software handling, the deuteron spectrum shown in Fig. 1 is from a run taken in an earlier phase of the experiment. The  $(d, d')$  spectra with the 3.3 keV FWHM resolution looks very similar to the proton spectra.] Free fits at the different scattering angles determined essentially all levels seen in proton scattering and vice versa. Part of the cross-section angular distributions are shown in

Figs. 2 and 3. For  $\alpha$  scattering the resolution was limited to 8 to 10 keV FWHM line width. This was sufficient to determine within DWBA or CC calculations collective transition strengths for the stronger natural parity transitions [34] and to provide some information about weaker excited states.

## B. Transfer reactions

For the  $^{207}\text{Pb}(d, p)^{208}\text{Pb}$  transfer measurements, the polarized deuteron beam from a Lamb shift ion source (intensity 150 nA, polarization parallel to the scattering normal  $P_y=0.60$ ) [36] has been used. Because of the spin filter in the source, the change of the direction of the polarization does not cause any changes of the beam position at the target. Figure 4 shows a typical spectrum. Angular distributions of differential cross section  $\sigma(\theta)$  and analyzing power  $A_y(\theta)$  for strong transitions above  $E_x=4$  MeV are shown in Fig. 5. Due to the relatively thick target (self-supporting 291  $\mu\text{g}/\text{cm}^2$  of  $^{207}\text{Pb}$  enriched to 99.81%) the resolution was in between 5 and 6 keV FWHM. The shapes of the angular distributions allow the assignment of transferred orbital ( $l$ ) and total ( $j$ ) angular momenta for the stronger transitions in transfer (see Fig. 5). For transitions with  $l>0$  and because of the dominance of the Coulomb barrier, a positive analyzing power is observed for transitions with  $j=l-1/2$  and a negative one for  $j=l+1/2$ . These angular distributions are easily reproduced in DWBA calculations [37] used for the respective potentials parameters which are close to those recommended in the literature [22,38–40]. With the identification of strong transitions in scattering and the determination of quantum numbers from the angular distributions in transfer for part of the transitions, we have succeeded to relate the energies of the levels in transfer to those in scattering and to the energies from  $\gamma$  spectroscopy, referring especially to the recent studies of Schramm *et al.* [1] and of Radermacher *et al.* [8].

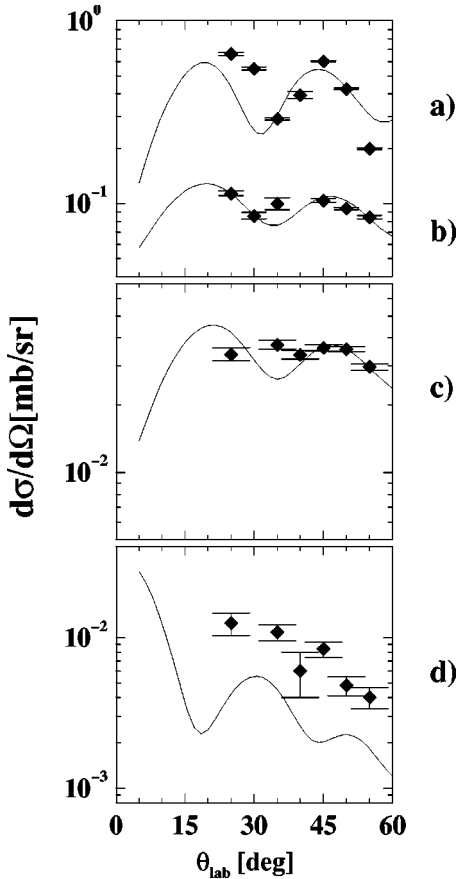


FIG. 2. Inelastic deuteron scattering angular distributions for (a) the  $2_1^+$  state ( $E_x=4085.4(3)$  keV,  $\beta_2=0.055$ ); (b) and (c) two relatively strongly excited higher lying  $3^-$ ; (b)  $E_x=6009.6(6)$  keV,  $\beta_3=0.033$ ; (c)  $E_x=5245.6(15)$  keV,  $\beta_3=0.0185$ ; and (d) the TOP  $0^+$  state ( $E_x=5240.8(15)$  keV,  $\beta_3=0.105$ ). The solid curves are from coupled channels calculations (code ECIS); the transition form factors are derived from the scattering potential with  $\beta_\lambda$  as normalization. For the  $0^+$  state, the calculation is as for a pure TOP state in a pure two-step excitation.

All levels observed in transfer show up in proton (and deuteron) scattering. Table I summarizes up to  $E_x=6100$  keV the observed excitation energies, the values of the differential cross sections in  $(p,p')$  and  $(d,p)$  at typical scattering angles, and the neutron transfer orbitals and strengths, if identified. A state is considered as observed if its  $(p,p')$  cross section is at least  $1 \mu\text{b/sr}$ , which is a factor of 1000 smaller than the excitation cross section of the strongest  $3_1^-$  state. As reference, the compilation of Schramm *et al.* [1] and the adopted levels of the Nuclear Data Sheets [21] are used. Results for higher energies up to  $E_x=7300$  keV are listed in Ref. [27].

### III. QPM CALCULATIONS

Recently, QPM calculations on a larger phonon (ph) basis in  $^{208}\text{Pb}$  have been performed with the main focus on the TOP states [41]. These calculations have been extended for the present studies to consider the model predictions of properties of all excited states with spin and parity from  $0^\pm$  to  $7^\pm$

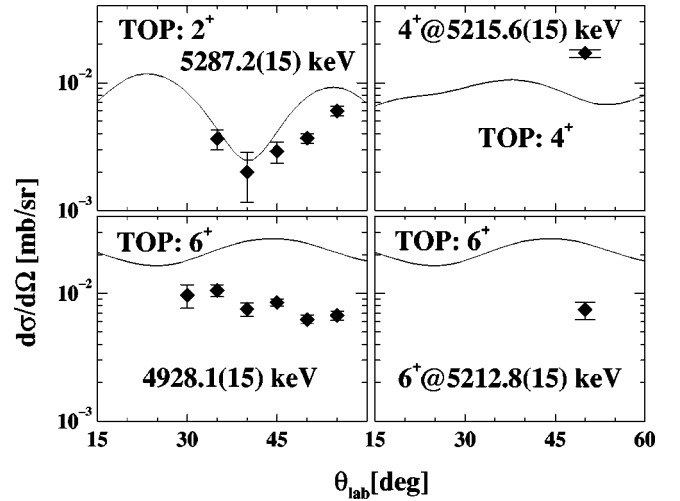


FIG. 3. Experimental  $(d,d')$  angular distributions of TOP candidates in comparison with predictions in the coupled channel approach. The comparison of the  $4928.1(15)$  keV state data with a  $6^+$  TOP calculation is tentative (see text).

and  $8^+$  up to the excitation energy of 8 MeV. They have been described by wave functions that include 1ph, 2ph, and 3ph configurations. Phonons with the above-mentioned multiplicities have been included in a model space. Their properties, i.e., excitation energies and internal fermion structure, are obtained by solving the RPA equations. Among them, there are indeed not only collective but weakly collective and practically pure 1p1h excitations. Multiphonon configurations are built up of all different combinations of phonons allowed by angular momentum coupling rules.

When two-phonon configurations are considered, their internal fermion structure is taken into account by applying exact (not bosonic) commutation relations between phonon operators. It means that although we describe nuclear excitations in terms of quasibosons (phonons), the wave functions of multiphonon states are antisymmetrized. The exclusion of the spurious np–nh configurations that violate Pauli's principle leads to a reduction of the collectivity of the

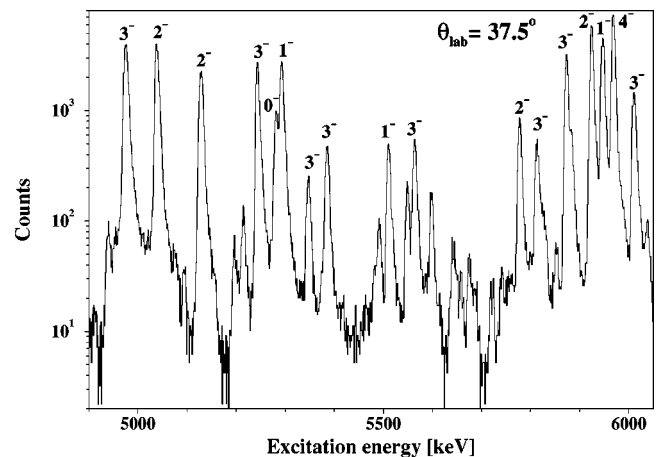


FIG. 4. Part of a  $^{207}\text{Pb}(d,p)^{208}\text{Pb}$  spectrum as function of the excitation energy in  $^{208}\text{Pb}$ . Safely assigned quantum numbers are indicated. Note the excitation of negative parity states only.

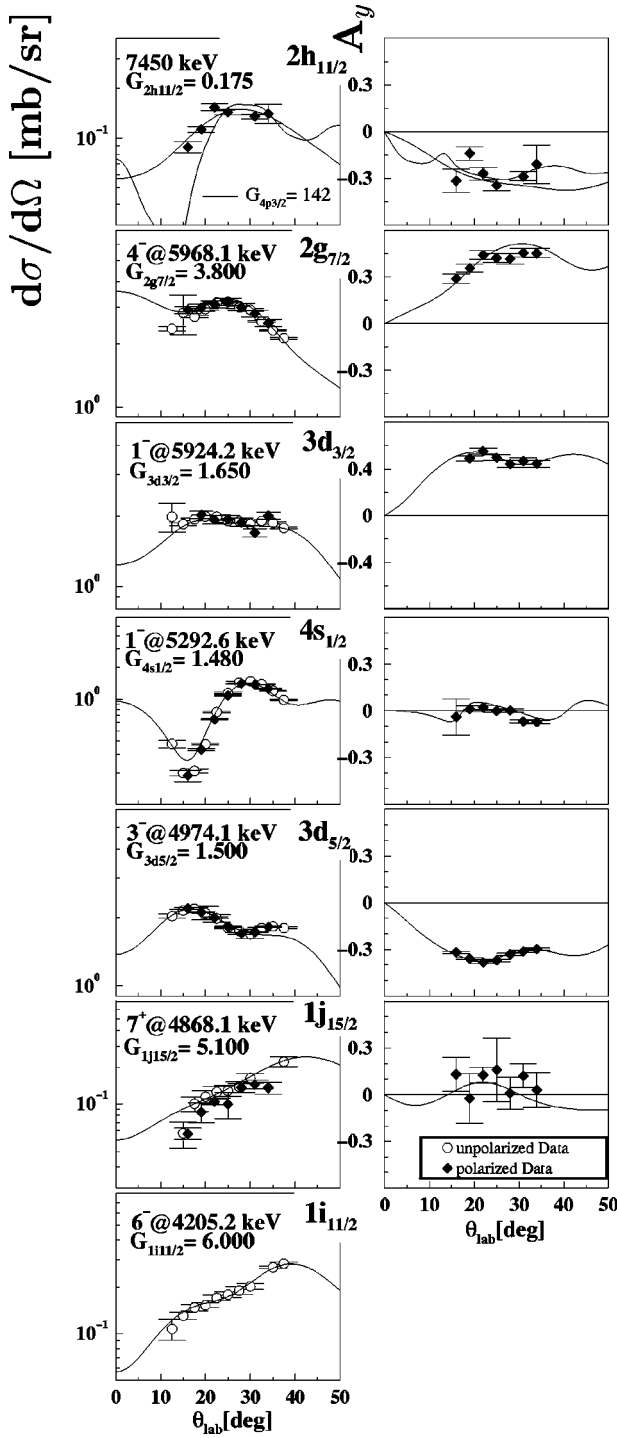


FIG. 5. A selection of measured  $^{207}\text{Pb}(d,p)^{208}\text{Pb}$  transfer angular distributions of differential cross section  $\sigma(\theta)$  and of analyzing power  $A_y(\theta)$  for strong transitions for different transferred  $l, j$  values at excitation energies above  $E_x=4000$  keV, as indicated. The respective curves are DWBA calculations assuming transfer in the neutron orbit indicated. The spectroscopic factors  $G_{lj}$  are indicated, which result from the normalization of the calculation to the data.

$n$ -phonon states. Since the low-lying states are made up of isoscalar phonons, Pauli principle corrections tend to increase the excitation energies of multiphonon states in respect to the harmonic limit.

The most essential difference of the present QPM calculations from the ones in Ref. [41] (in addition to a larger model space) is the single-particle spectrum employed. In Ref. [41] the single-particle energies of the average field near the Fermi surface have been taken from experimental data. In these studies they have been varied to describe in the neighboring  $^{207}\text{Tl}$ ,  $^{207,209}\text{Pb}$ , and  $^{209}\text{Bi}$  nuclei with an accuracy of 10 keV the experimental excitation energies of levels with predominant 1p (or 1h) structure in calculations, where the wave functions also include “1p(1h)  $\otimes$  1ph” configurations. In the calculations of the odd nuclei the phonons belong to the  $^{208}\text{Pb}$  core.

In the present calculations, the phonons are determined by three parameters. The first two parameters are the strength of the isoscalar residual interaction of the model Hamiltonian for positive and negative natural parity states adjusted to reproduce collective properties, i.e.,  $B(E\lambda)$  values, and excitation energies of the  $2_1^+$ ,  $4_1^+$ , and  $6_1^+$  ( $3_1^-$  and  $5_1^-$ ) states in  $^{208}\text{Pb}$ . The third parameter is the strength of the residual interaction for all unnatural parity states determined to describe the energy of the  $M1$  resonance. With this procedure we achieve a self-consistent description of  $^{208}\text{Pb}$  and its four odd-mass neighbors.

Results for  $^{208}\text{Pb}$  have been obtained by diagonalization of the QPM Hamiltonian on a set of wave functions that include coupling between 1ph, 2ph, and 3ph configurations. Performing calculations, we have truncated 1ph and 2ph configurations above 10 MeV and 3ph configurations above 12 MeV. The diagonalization yield eigenenergies and eigenvectors. Thus the information on a contribution of any configuration from the model space to the structure of each excited state is available. Since the internal fermion structure of phonons is also known, calculation of the spectroscopic factors  $G_{lj}$  for a comparison with the data from the  $(d,p)$  reaction is rather straightforward. The results of calculations are summarized in Table II. As in Table I, they are presented up to the excitation energy of 6.1 MeV. Theoretical predictions up to 8 MeV are available [42].

A comparison of Tables I and II shows a very good correspondence between experimental data and the QPM predictions of the energy spectrum. More detailed comparison will be presented below.

## IV. CONFIGURATION MIXING AND LEVEL DENSITY

### A. Spectroscopic factors

Most levels observed in transfer show angular distributions allowing the assignment of definite  $lj$  values of transferred angular momentum.

Because of the angular momentum  $p_{1/2}$  of the target, a final state  $J^\pi = j \pm 1/2$  may be populated by two different values of  $j$  transfer. For natural parity states they differ by two units in orbital angular momentum  $l = J \pm 1$ ; for unnatural parity states they are the same, i.e.,  $l = J$ . The polarization dependent cross sections of the two  $j$  transfers add incoherently, thus their relative contributions are easily obtained from a fit of the data using DWBA curves with potentials adjusted to reproduce strong transitions where one configuration dominates [27].

TABLE II. Excitation energies,  $E_x$ , and spectroscopic factors,  $G_{ij}(nlj)$  of low-lying states in  $^{208}\text{Pb}$  up to 6.1 MeV from QPM calculations. Spectroscopic factors less than 0.01 are not indicated. Index  $\nu$  means the first, second, etc. excited state for each multipolarity. States that have predominantly two-phonon nature are indicated by “\*.” Among the last, there are the TOP states, presented separately in Table III, and other lowest two-phonon states,  $[3_1^- \times 5_1^-]_{J^+}$  and  $[5_1^- \times 5_1^-]_{J^+}$ .

$J^\pi$	$\nu=$	1	2	3	4	5	6	7	8	9	10	11	12	13
$0^+$	$E_x$ [MeV]	5.34*	6.11*											
$1^-$	$E_x$ [MeV]	5.28	5.64	5.94	6.02	6.09								
	$G_{ij}(4s_{1/2})$	1.45												
	$G_{ij}(3d_{3/2})$			1.29	0.01	0.07								
$2^+$	$E_x$ [MeV]	4.13	5.15*	5.45	5.55*	5.71	6.11*							
$3^-$	$E_x$ [MeV]	2.57	4.07	4.32	4.50	4.88	5.13	5.41	5.61	5.70	5.96	6.00	6.03	6.11
	$G_{ij}(3d_{5/2})$	0.09			0.02	1.99	1.20	0.07	0.01	0.03				
	$G_{ij}(2g_{7/2})$	0.09				0.04	0.06	0.07	0.07	0.22	0.36	1.15	0.57	0.54
$4^+$	$E_x$ [MeV]	4.34	5.24*	5.40	5.55*	5.66	6.08*							
$5^-$	$E_x$ [MeV]	3.14	3.67	3.94	4.03	4.14	4.43	4.54	4.95	5.35	5.68	5.93		
	$G_{ij}(2g_{9/2})$	3.33	1.98		0.03	0.02	0.01	0.01	0.01	0.04		0.01		
	$G_{ij}(1i_{11/2})$	0.40	1.12	2.50	1.14	0.14	0.05		0.01	0.06		0.01		
$6^+$	$E_x$ [MeV]	4.44	5.15	5.40	5.55*	5.64	5.69	6.03	6.08					
$7^-$	$E_x$ [MeV]	3.95	4.54	4.89	5.85									
$8^+$	$E_x$ [MeV]	4.58	5.03	5.31	5.48	5.66	5.85	5.95*						
	$G_{ij}(1j_{15/2})$	5.40	1.46	0.28	0.09	0.01	0.29	0.20						
$0^-$	$E_x$ [MeV]	5.28*	5.71*											
	$G_{ij}(4s_{1/2})$	0.48												
$1^+$	$E_x$ [MeV]	5.82												
$2^-$	$E_x$ [MeV]	4.19	5.02	5.59	5.65	5.92	6.05	6.09						
	$G_{ij}(3d_{5/2})$	0.03	2.38	0.01										
	$G_{ij}(3d_{3/2})$					2.36	0.01	0.02						
$3^+$	$E_x$ [MeV]	5.16	5.49	5.80*	5.83									
$4^-$	$E_x$ [MeV]	3.46	4.04	4.11	4.45	4.56	5.32	5.48	5.63	5.90	5.95	6.09		
	$G_{ij}(2g_{9/2})$	4.31	0.03		0.02	0.01								
	$G_{ij}(2g_{7/2})$										4.28			
$5^+$	$E_x$ [MeV]	5.13	5.40	5.66	5.80*	5.85								
$6^-$	$E_x$ [MeV]	3.93	4.05	4.11	4.56	4.60	4.96	5.96						
	$G_{ij}(1i_{11/2})$	6.43												
$7^+$	$E_x$ [MeV]	4.93	5.21	5.37	5.58	5.73	5.80*	5.99	6.06					
	$G_{ij}(1j_{15/2})$	6.36	0.19		0.03	0.01	0.03		0.03					

From these fits, spectroscopic factors  $G_{ij}^J$  ( $G_{ij}^J = (2j+1)S_{ij}$ , see Ref. [43]) result. Their distributions over the individual states are shown in Fig. 6; for weak states this figure includes few tentative assignments.

For each transferred orbital  $nlj$  most of the strength is concentrated in a few nearby states; the identified values of strength range, however, over three orders of magnitude. The respective long tails of the strength distributions reflect the amount of mixing in between the  $1p1h$  configurations. From the apparent admixture of small components, to any state with the respective quantum number follows that all states with these quantum numbers should be seen in  $(d,p)$  with some cross section, irrespective of whether the cross sections are large enough to determine quantum numbers.

The summed spectroscopic factors can be compared with those, deduced from transfer on a  $^{208}\text{Pb}$  target at the same energy at a few scattering angles [27]. Most of them agree within an experimental uncertainty of  $\pm 5\%$ . At higher excitation energies beyond the strong  $2g_{7/2}$  and  $3d_{3/2}$  single par-

ticle transitions in  $^{209}\text{Pb}$  the spectrum shows only weakly distributed strength, which originates predominantly from the coupling of a valence neutron to excited core configurations.

The plot in Fig. 6 extends to the neutron emission threshold.  $2g_{9/2}$ ,  $1i_{11/2}$ ,  $1j_{15/2}$ ,  $3d_{5/2}$ ,  $4s_{1/2}$ ,  $2g_{7/2}$ , and  $3d_{3/2}$  configurations exhaust their  $(2j+1)$  limits up to this energy. This agreement, however, depends on the choice of the neutron single particle potential. No attempt was made to determine absolute values of spectroscopic factors.

Incremental plots of the spectroscopic factors predicted by the QPM calculations are shown in Fig. 6 by dashed lines to be compared with incremental plots from the present data analysis (solid lines). One may notice an excellent agreement in the energy position of the states exhausting the main fraction of the spectroscopic strength of the respective single-particle configuration. The QPM also reproduce well a stronger fragmentation of the  $3d_{3/2}$ ,  $2g_{7/2}$ , and  $3d_{5/2}$  configurations and concentration of other configurations in

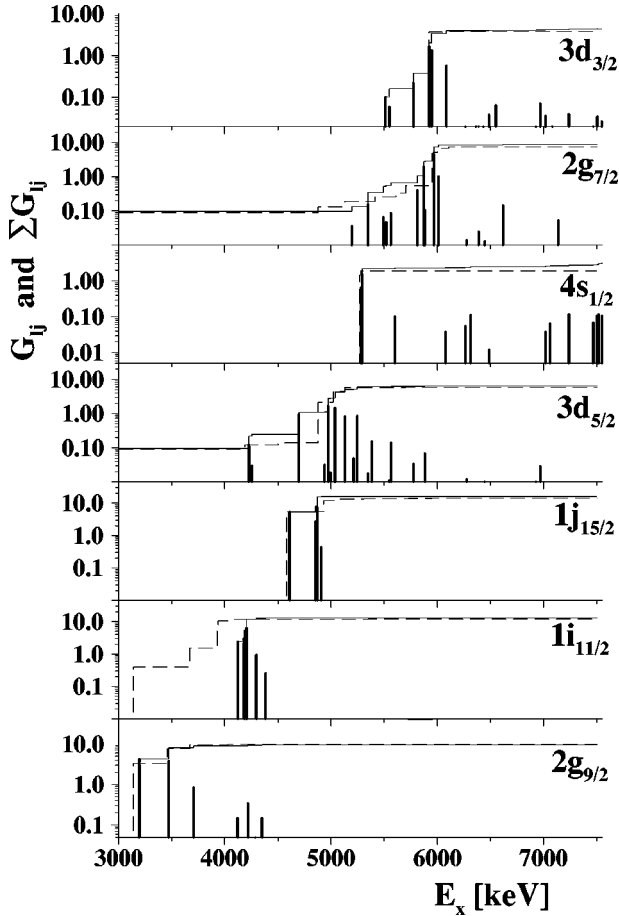


FIG. 6. The spectroscopic factors  $G_{ij}$  of states in  $^{208}\text{Pb}$  from the  $^{207}\text{Pb}(\bar{d},p)^{208}\text{Pb}$  reaction in differential and incremental (solid lines) presentation. Incremental plots of the spectroscopic factor predicted by the QPM calculations are shown for comparison by dashed lines. Note the logarithmic scale.

only few excited states. Low-energy tails in the QPM predictions for the  $3d_{5/2}$  and  $2g_{7/2}$  configurations are due to the presence of these configurations in the collective  $3_1^-$  state, not included in the present analysis. Experimental spectroscopic factors for these states in Fig. 6 are taken from Ref. [1].

### B. Level density

To answer the question whether we observe all states in this range, we compare the observed level densities in transfer and scattering with model expectations. In Fig. 7, we plot as function of the excitation energy the incremental number of states observed in  $(d,p)$  and in  $(p,p')$  and compare with the respective numbers of expected 1p1h states. Since we are interested here in the number of observed states only, we neglect the mixing between the 1p1h configurations. Thus we use for the expected excitation energies those of the respective pure 1p1h multiplets at their unperturbed energies, as they result from the experimental spectra of the  $A=207$  and  $209$  nuclei, summarized in Fig. 1 of Warburton and Brown [44]. With respect to the selectivity of the reactions discussed above, we include for  $(p,p')$  all states up to an-

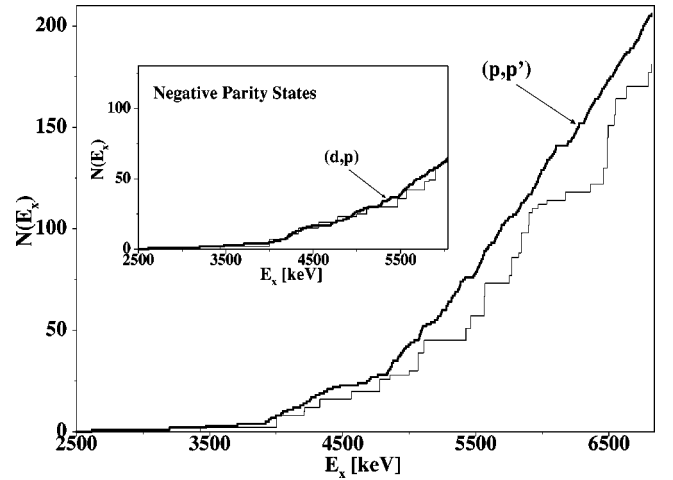


FIG. 7. Incremental plot of the number of states in  $^{208}\text{Pb}$  as observed in  $(d,p)$  and  $(p,p')$ , respectively, compared with an expectation, considering the 1p1h states at their unperturbed energies only and applying restrictions about the observation of quantum numbers as described in the text.

gular momentum transfer  $l=10\hbar$ ; and for  $(d,p)$  the negative parity states only up to  $l=6\hbar$ , the identified  $j_{15/2}$  and tentatively identified  $h_{11/2}$  are omitted in this part of the figure. For  $(p,p')$  the range of excitation energies is up to  $E_x=6800$  keV, about twice the minimal energy of a pure 1p1h excitation, and for  $(d,p)$  comparison ranges up to  $E_x=6030$  keV to avoid complications as discussed for  $h_{11/2}$  transfer.

For  $(d,p)$  the agreement is very good, indicating that we observe essentially all negative parity states (up to  $J=6$ ). For  $(p,p')$  the number of observed states is larger than the number of expected 1p1h states. This is in qualitative agreement with the downshift of some 1p1h states due to collectivity, and with the additional contributions of 2p2h states which are lowered in excitation energy due to collectivity. Candidates in this energy range are (compare Fig. 5 in Schramm *et al.* [1] and for further reference, e.g., the studies of Blomqvist [20] and Ring and Schuck [18]) one neutron and one proton monopole pairing vibrational (MPV)  $0^+$  state, with the neutron-MPV state observed at 4867 keV; two neutron and two proton quadrupole pairing vibrational (QPV)  $2^+$  states, starting from 5551 keV and identified in part from two nucleon transfer (e.g. Grabmayr *et al.* [45]); four TOP states  $0^+$ ,  $2^+$ ,  $4^+$ ,  $6^+$  near  $E_x=2 \times E_x(3_1^-)=2614.5$  keV = 5229 keV; seven states from  $2^+$  to  $8^+$  near  $E_x=5812$  keV, resulting from the coupling of the collective  $3_1^-$  state at  $E_x=2614.5$  keV with the collective  $5_1^-$  state at  $E_x=3197.7$  keV state, and so on.

In  $^{208}\text{Pb}$ , the number of low-lying states with spin and parity equal to  $3^-$  and  $5^-$  is especially large. Their spectra are compared in Fig. 8 with prediction of the microscopic QPM calculations. There are 21  $3^-$  states below 7 MeV in both experiment and calculation and 14  $5^-$  states observed while QPM predicts three more excited states. Due to high energy of the  $2_1^+$  and  $4_1^+$  states, negative parity states that have predominant two-phonon nature do not appear in  $^{208}\text{Pb}$  below 6.7 MeV. A general agreement between experimental and calculated spectra of the  $3^-$  and  $5^-$  states is very good,

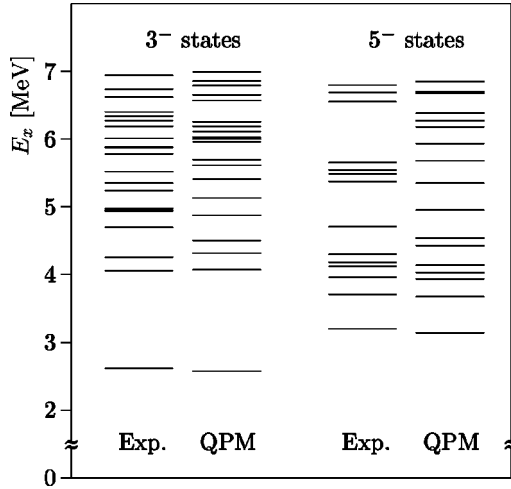


FIG. 8. Comparison between QPM calculation and experimental data of excitation energies of  $3^-$  and  $5^-$  states in  $^{208}\text{Pb}$ .

as seen from Fig. 8. An agreement for the states of other multipolarities in excitation energies and density of states is of the same quality, as maybe concluded from a detailed comparison of Tables I and II. This is because a complete phonon basis is used in calculations, and we employ a good single-particle spectrum that is well known to high excitation energies from the  $A=207$  and  $209$  nuclei. From these comparisons, we conclude that  $(p,p')$  and  $(d,d')$  scattering show essentially all states up to  $E_x=6$  MeV.

## V. DOUBLE OCTUPOLE CANDIDATES AND SCATTERING ANGULAR DISTRIBUTIONS

Since in  $^{208}\text{Pb}$  the  $3_1^-$  level is the lowest in energy, the lowest two-phonon states in this nucleus are expected to belong to the two octupole phonon (TOP) multiplet representing the  $[3_1^- \otimes 3_1^-]_{0^+, 2^+, 4^+, 6^+}$  configurations. In the harmonic picture of nuclear excitation, and the  $3_1^-$  state is known to be the most collective state in  $^{208}\text{Pb}$ , this multiplet is expected at the twice the energy of the  $3_1^-$  level, i.e., around 5229 keV. Unfortunately, there is no nuclear reaction selective to the excitation of the TOP states. That is why different tools  $[(n,n'\gamma\gamma)$  reaction [6,7], nuclear resonance fluorescence studies [15], inelastic light particle scattering [13], heavy ion induced reactions [9,11,12]] have been used in the past for its identification.

In spite of these tremendous experimental efforts only the  $0^+$  component of the TOP has been assigned as the  $0_2^+$  state at  $E_x=5241$  keV, which is very near to the harmonic limit, by its two sequential  $E3$  transitions to the ground state [6]. Inelastic light particle scattering supports the TOP purity of the  $0_2^+$  state due to the observed excitation strength [14]. Since the branching ratios of the collective  $E3$  decays of the  $2^+$ ,  $4^+$ , and  $6^+$  TOP configurations into the  $3_1^-$  state are smaller than the ones for the noncollective  $E1$  decay into the  $3_1^-$  or  $5_1^-$  states, the strongest low-energy  $E1$  transitions have been used to propose the  $2^+$  state at  $E_x=5286$  keV and the  $4^+$  state at 5216 keV as the TOP candidates in Ref. [4]. But theoretical estimates of the  $E1$  transitions between one-

phonon configurations in this energy region showed that observed strong  $E1$ -intensities cannot be used as a signature of  $[3_1^- \otimes 3_1^-]_{2^+, 4^+, 6^+} \rightarrow 3_1^-$  decay [41]. On the other hand, inelastic light particle scattering ruled out strong TOP strength for a  $4^+$  or  $6^+$  state at 5683 keV (because of low cross sections) [13], which had been suggested from observations in heavy ion induced reactions [11,12].

While the recent QPM calculations [41] predict that the  $0^+$ ,  $2^+$ , and  $4^+$  members of the TOP multiplet are essentially concentrated in single states, not far from the harmonic limit, they also indicate that the  $[3_1^- \otimes 3_1^-]_{6^+}$  configuration is strongly fragmented over a wide energy region. The latter aspect has been confirmed in recent heavy ion induced reactions [9], with 20% of the strength found in the  $6_1^+$  state at 4423 keV. This experiment has also given the upper limit for the TOP configuration 15% in the state near 5200 keV and a TOP tail spreading up to 6 MeV.

The inelastic scattering angular distributions are sensitive also to features of two phonon collectivity, as they are described in the Tamura formalism in the case of coupled channels (CC) [30,33]. As reported above, complete spectroscopy predict only a few  $0^+$ ,  $2^+$ ,  $4^+$ , and  $6^+$  levels in 1 MeV energy region centered around the TOP harmonic limit. Their  $(d,d')$  scattering angular distributions will be examined in this section to conclude information of TOP strength in these states.

## A. Spectra

Short ranges of the excitation spectra near the undisturbed double octupole energy at 5229 keV are shown in Fig. 1 for  $(p,p')$ ,  $(d,d')$ , and  $(\alpha,\alpha')$  scattering. All states known from literature in this energy region are observed. There are eight additional ones in this range, indicated in the top of Fig. 1 in gray shading. Three of eight newly detected levels have very low cross sections near  $1 \mu\text{b}/\text{sr}$ , and are not further considered. The remaining five have cross sections comparable to the line at  $E_x=5240.8$  keV (filled with black), which is because of the precisely defined excitation energy (note the nearby  $E_x=5245.5$  keV  $3^-$  state) identified as the  $0_2^+$  state of Yeh *et al.* [6], the proposed  $0^+$  member of the TOP multiplet. These five states are not resolved in  $(\alpha,\alpha')$  scattering, but they are in ranges with large cross sections. Thus not in contradiction with natural parity, the resolution does not allow for more definite conclusions. Of those states, the ones at  $E_x=5079$ , 5088, and 5287 keV do not show up in  $(d,p)$ ; this excludes negative parity and provides with the presumed natural parity evidence for three new states which are likely to have  $2^+$ ,  $4^+$ , or  $6^+$ . The same arguments hold for an isolated, undoubtedly identified state at  $E_x=4928.1$  keV, which because of the energy may be equated with the 4923? keV state of Refs. [21,46] discussed there as the  $2^+$  member of the TOP multiplet.

With the above-mentioned  $0^+$  state at 5240.8 keV, the known  $6^+$  state at 5212.8 keV, and the  $4^+$  state at 5215.6 keV, these are the candidates for TOP excitation or mixing with the respective TOP configurations. Including the well known  $0_1^+$ ,  $2_1^+$ ,  $4_1^+$ , or  $6_1^+$  states at 4866.8, 4085.4, 4323.9, and 4422.6 keV, respectively, these are the identified and

presumably all of the excitations with the TOP quantum numbers at an energy approximately below 5300 keV.

**B. Angular distributions**

Angular distributions, as obtained from the  $(d,d')$  spectra, are compared in this subsection with model calculations. The angular distributions of the collective  $2_1^+$  state and of two relatively strongly excited  $3^-$  states near the TOP energy (the  $3_1^-$  state was outside the acceptance range of the magnetic spectrometer), shown in the upper part of Fig. 2, are reproduced fairly well in coupled channels (CC) calculation. They use optical potentials and the vibrational collective model with strength amplitudes  $\beta_\lambda$  as parametrization of the transition form factors, as discussed in detail in Ref. [32]. With the code ECIS [47] and an optical potential very near to recommended global parameterization of Ref. [22,40], these distributions are reproduced with values for  $\beta_\lambda$  very near to those given in the literature [22,34].

The TOP cross sections are calculated as two step sequential excitations of pure TOP states with the  $\beta_3$  value for the collective  $3_1^-$  excitation of  $\beta_3=0.105$  [22]. For the  $0^+$  TOP state, the result is shown in the lower part of Fig. 2 and compared with our data. The relative angular dependence of the cross section data of the known  $0_2^+$  state at 5240 keV is in approximate agreement with the calculation; the absolute values, however, exceed the TOP calculation by a factor of 2. The respective calculations for pure  $2^+$ ,  $4^+$ , and  $6^+$  TOP states are shown with data for known or tentatively assigned states in Fig. 3. These calculated cross sections of about 10  $\mu\text{b/sr}$  are rather low.

For the proposed  $2^+$  state at 5287 keV, the TOP calculation reproduces the relative angular dependence rather well. The observed absolute values are about 80% of the calculated ones.

The cross section of the known  $4^+$  state at 5215 keV is difficult to separate from the cross section of the known  $6^+$  state at 5212 keV. The only data point we have is at  $\theta = 50^\circ$ . The experimental  $4^+$  cross section exceeds the calculated TOP cross section by a factor of 2, whereas the  $6^+$  state is observed with only about 30% of the calculated TOP cross section.

In Fig. 3 we also show data for the 4928 keV state, which was introduced by Mariscotti [21,46] as a  $2^+$  state. But this assignment, as well as the assignments for further low lying  $2^+$  states listed in NDS, was not confirmed in the work of Schramm *et al.* [1]. Also, our observed angular dependence is not in agreement with a one step or two step  $2^+$  excitation.

In Fig. 9 we compare the results of our present QPM calculations of the low energy part of the  $0^+$ ,  $2^+$ ,  $4^+$ , and  $6^+$  spectra, excitation energies, and TOP strengths, with experimental knowledge and our observations. Since we have used in these calculations slightly different single particle spectra and strengths of the residual interaction, as compared to the ones in Ref. [41] (see above), details of the TOP state properties have changed, too. Nevertheless, the changes are not very essential, as may be concluded by comparing the

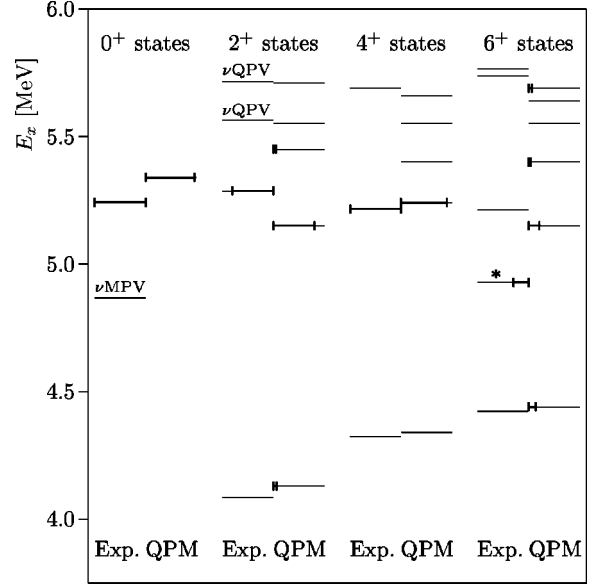


FIG. 9. Observed states of positive and natural parity in  $^{208}\text{Pb}$  and their strength, as obtained from the comparison of  $(d,d')$  cross sections and TOP coupled channel calculations (depicted for each spin on the left hand side) in comparison with calculated states and their predicted TOP strength by QPM calculation (for each spin on right). The assignment of the 4928.1(15) keV state as  $6^+$  (marked with an asterisk) is tentative.

results presented in Table III with similar results in Table II in Ref. [41].

For the  $0^+$ ,  $2^+$ , and  $4^+$  states, calculations predict concentration of the TOP strength in one state near 5230 keV, the harmonic limit, and spreading of the  $6^+$  TOP strength over a number of states, each bearing only up to 20% of the  $6^+$  TOP strength. The concentration of the  $0^+$ ,  $2^+$ , and  $4^+$  TOP strength in essentially one state is related with the re-

TABLE III. Fragmentation of the TOP configurations  $[3^-1 \times 3^-1]_{0^+,2^+,4^+,6^+}$  over low-lying states in  $^{208}\text{Pb}$ . Only states with a TOP contribution larger than 3% are presented. The third column gives the TOP contribution to the wave functions. The fourth column is the largest component of other one- or two-phonon configurations.

$\lambda_\nu^\pi$	$E_x$ [MeV]	TOP	Other
$0_1^+$	5.34	95.8%	< 1%
$2_1^+$	4.13	6.2%	$2^+1 - 91.8\%$
$2_2^+$	5.15	80.2%	$2^+2 - 5.7\%$
$2_3^+$	5.45	5.7%	$2^+2 - 89.8\%$
$4_2^+$	5.24	90.5%	$4^+1 - 1.9\%$
$6_1^+$	4.44	14.1%	$6^+1 - 80.7\%$
$6_2^+$	5.15	21.7%	$6^+2 - 33.4\%$
$6_3^+$	5.40	3.9%	$6^+2 - 58.7\%$
$6_6^+$	5.69	6.5%	$6^+5 - 40.4\%$
$6_7^+$	6.03	15.3%	$6^+6 - 49.3\%$
$6_8^+$	6.08	14.2%	$6^+6 - 44.0\%$
$6_9^+$	6.15	13.1%	$[5^-1 \times 5^-1]_{6^+} - 61.8\%$

spective low level density. In fact, these TOP dominated  $0^+$ ,  $2^+$ , and  $4^+$  states are obtained as the second excited states  $0_2^+$ ,  $2_2^+$ ,  $4_2^+$ , following the neutron pairing monopole vibrational state ( $\nu\text{MPV}$ , which is outside the multiphonon space used in the calculation) and the low lying, collectively enhanced  $2_1^+$ ,  $4_1^+$  states. For  $6^+$  there are more nearby states to mix, and TOP strength in the 20% range is predicted for the collective enhanced  $6_1^+$  state around 4.4 MeV, the  $6_2^+$  state around 5.2 MeV and  $6_{7,8,9}^+$  states between 6.0 and 6.2 MeV.

Our observed large cross sections for the  $0_2^+$  state at 5240 keV, the  $2^+$  state at 5287 keV, and the  $4_2^+$  state at 5215 keV are in agreement with the calculations. Our observation of a rather pure TOP  $2^+$  state gives strong support to the calculation and implies the nonexistence of another nearby  $2^+$  state. Thus we identify the 5287 keV  $2^+$  state as the  $2_2^+$  state and thus rule out an  $2^+$  assignment for the 4928 keV state. Our weak observed  $6^+$  cross section for the state at 5212 keV is in agreement with the weak predicted TOP strength of these states, it is either the calculated  $6_2^+$  state near 5150 keV or the  $6_3^+$  state near 5400 keV. Identifying the experimental 5212 keV state as  $6_3^+$ , one may ask whether the 4928 keV state can be identified with the calculated  $6_2^+$  state near 5150 keV. In Fig. 3, the observed angular dependence is consistent with a  $6^+$  TOP calculation and a 30% TOP strength. This, however, is a completely tentative assignment.

At present, we have to limit the interpretation of these weak cross sections to a discussion of the respective order of magnitudes only. The main source of uncertainties is due to the limited accuracy in the CC calculations.

The calculated angular distributions depend on details, as the inclusion of additional one-step amplitudes that arise from configuration mixing with  $1p1h$  (one phonon) states (causing the spreading of the TOP strength, discussed above); and also due to the two phonon nature, being part of the formalism of pure two phonon excitations (compare Refs. [30,33]), examples are discussed in Ref. [32] for the excitations of  $6^+$  TOP states in scattering from  $^{96}\text{Zr}$  [48]. Because of the highly effective deuteron nucleus interaction at these low projectile energies (needed to resolve the states), a reliable folding of microscopic transition form factors from a multiphonon calculation (including all this features) in scattering amplitudes, and this for angular momentum transfers ranging from  $0^+$  to  $6^+$ , is difficult to obtain in a reliable way and is thus not considered in the present study.

Thus we conclude that the observed order of magnitude of the cross sections of these states are in agreement with the QPM calculation and the respective fragmentation of TOP strength. The incomplete angular distributions, as well as the

theoretical uncertainties, do not allow us to draw more conclusions.

## VI. SUMMARY

To identify the states of the  $0^+$ ,  $2^+$ ,  $4^+$  and  $6^+$  TOP multiplets in  $^{208}\text{Pb}$  and their respective fragmentation inelastic proton, deuteron and  $\alpha$  scattering have been measured in high energy resolution. Determination of quantum numbers and information about mixing between  $1p1h$  configurations is obtained from the  $^{207}\text{Pb}(d,p)^{208}\text{Pb}$  transfer reaction with vector polarized deuterons. From the comparison with literature and model expectations we conclude that up to  $E_x=6$  MeV essentially all states are resolved.

Our strength distributions, as obtained from the polarized  $(d,p)$  experiment, display in a direct way the strength of configuration mixing. This compares well with the determination of matrix elements as, e.g., in the most recent work of Schramm *et al.* [1].

Coupled channels calculations of the  $(d,d')$  scattering cross sections have been used to study those natural and positive parity states that may belong to the TOP multiplet in  $^{208}\text{Pb}$ . The angular distributions for the  $0^+$  state at 5240 keV, the  $2^+$  state at 5287 keV, and the tentatively assigned  $6^+$  state at 4928 keV agree well with the assumption of a two-step mechanism, an excitation by two sequential  $E3$  transitions. Unfortunately, the limited accuracy in the calculation of these weak cross sections does not allow to conclude precisely on the purity of the TOP configurations in the above-mentioned states.

Microscopic QPM calculations of the properties of excited states in  $^{208}\text{Pb}$  up to 8 MeV in a practically complete phonon basis, which includes one- and multiphonon configurations, are performed and compared with the properties of levels from the present experimental studies. The general agreement between experiment and theory in the number of excited states, their excitation energies and spectroscopic factors are very good.

## ACKNOWLEDGMENTS

For encouragement and stimulating discussions the authors thank Dr. P. von Brentano, Dr. T. Faestermann, Dr. P. Garrett, Dr. K. H. Maier, Dr. P. von Neumann-Cosel, and Dr. S. Yates. They also thank Dr. H. J. Maier *et al.* for preparation of the target, the Beschleunigerlaboratorium der Universität München und der Technischen Universität, and the DFG under IIC4 Gr 894/2. V.Yu.P. acknowledges support from NATO and the DFG Grant No. Rus 17/80/99.

- [1] M. Schramm, K.H. Maier, M. Rejmund, L.D. Wood, N. Roy, A. Kuhnert, A. Aprahamian, J. Becker, M. Brinkman, D.J. Decman, E.A. Henry, R. Hoff, D. Manatt, L.G. Mann, R.A. Meyer, W. Stoeffl, G.L. Struble, and T.-F. Wang, Phys. Rev. C **56**, 1320 (1997).  
 [2] M. Schramm, M. Rejmund, K.H. Maier, H. Grawe, and J. Blomqvist, Phys. Scr. **T56**, 307 (1995).

- [3] M. Schramm, Ph.D. thesis, Hahn-Meitner-Institut Berlin GmbH, Berlin, 1993.  
 [4] M. Yeh, M. Kadi, P.E. Garrett, C.A. McGrath, S.W. Yates, and T. Belgya, Phys. Rev. C **57**, R2085 (1998).  
 [5] S.W. Yates, M. Yeh, M. Kadi, C.A. McGrath, P.E. Garrett, and T. Belgya, J. Phys. G **25**, 691 (1999).  
 [6] M. Yeh, P.E. Garrett, C. McGrath, S.W. Belgya, and S.W.

- Yates, Phys. Rev. Lett. **76**, 1208 (1996).
- [7] M. Yeh, P.E. Garrett, C.A. McGrath, and S.W. Yates, Phys. Rev. C **54**, 942 (1996).
- [8] E. Radermacher, M. Wilhelm, S. Albers, J. Eberth, N. Nicolay, H.G. Thomas, H. Tiesler, P. von Brentano, R. Schwengner, S. Skoda, G. Winter, and K.H. Maier, Nucl. Phys. **A597**, 408 (1996).
- [9] K. Vetter, A.O. Macchiavelli, D. Cline, H. Amro, S.J. Asztalos, B.C. Busse, R.M. Clark, M.A. Deleplanque, R.M. Diamond, P. Fallon, R. Gray, R.V.F. Janssens, R. Krücken, I.Y. Lee, R.W. MacLeod, E.F. Moore, G.J. Schmid, M.W. Simon, F.S. Stephens, and C.Y. Wu, Phys. Rev. C **58**, R2631 (1998).
- [10] K. Vetter, A.O. Macchiavelli, S.J. Asztalos, R.M. Clark, M.A. Deleplanque, R.M. Diamond, P. Fallon, R. Krücken, I.Y. Lee, R.W. MacLeod, G.J. Schmid, and F.S. Stephens, Phys. Rev. C **56**, 2316 (1997).
- [11] H.J. Wollersheim *et al.*, Nuovo Cimento A **111**, 692 (1998).
- [12] H.J. Wollersheim, P. Egelhof, H. Emling, J. Gerl, W. Henning, R. Holzmann, R. Schmidt, R.S. Simon, N. Martin, G. Eckert, Th.W. Elze, K. Stelzer, R. Kulesa, G. Duchene, B. Haas, J.C. Merdinger, J.P. Vivien, J. de Boer, E. Hauber, K. Kaiser, P. von Brentano, R. Reinhardt, R. Wirowski, R. Julin, C. Fahlender, I. Thorslund, and H. Kluge, Z. Phys. A **341**, 137 (1992).
- [13] B.D. Valnion, W. Oelmaier, D. Hofer, E. Zanotti-Müller, G. Graw, U. Atzrott, F. Hoyler, and G. Staudt, Z. Phys. A **350**, 11 (1994).
- [14] B. D. Valnion, A. Gollwitzer, R. Hertenberger, A. Metz, P. Schiemenz, G. Graw, in *Capture Gamma Ray Spectroscopy and Related Topics*, Proceedings of the 9th International Symposium, 1996, edited by G.L. Molnar, T. Belgya, and Zs. Révay (Springer, New York, 1997), p. 329.
- [15] J. Enders, P. von Neumann-Cosel, V.Yu. Ponomarev, and A. Richter, Nucl. Phys. **A612**, 239 (1997); J. Enders, P. von Brentano, J. Eberth, A. Fitzler, C. Fransen, R.-D. Herzberg, H. Kaiser, L. Käubler, P. von Neuman-Cosel, N. Pietralla, V.Yu. Ponomarev, A. Richter, H. Schnare, R. Schwengner, S. Skoda, H.G. Thomas, H. Tiesler, D. Weisshaar, and I. Wiedenhöver, *ibid.* **A674**, 3 (2000).
- [16] A. Bohr and B. Mottelson, *Nuclear Structure Vol. II* (Benjamin, New York, 1975).
- [17] P. Schuck, Z. Phys. A **279**, 31 (1976).
- [18] P. Ring and P. Schuck, *The Nuclear Many-Body Problem* (Springer, New York, 1980).
- [19] T.T.S. Kuo, J.E. Blomqvist, and G.E. Brown, Phys. Lett. **31B**, 93 (1970).
- [20] J. Blomqvist, Phys. Lett. **33B**, 541 (1970); (private communication).
- [21] M.J. Martin, Nucl. Data Sheets **47**, 797 (1986).
- [22] H. Clement, Habilitation thesis, LMU, 1982 (unpublished).
- [23] V.G. Soloviev, *Theory of Atomic Nuclei: Quasiparticles and Phonons* (Institute of Physics, Bristol, 1992).
- [24] M. Loeffler, H.J. Scheerer, and H. Vonach, Nucl. Instrum. Methods **3**, 1 (1973).
- [25] E. Zanotti, M. Bisenberger, R. Hertenberger, H. Kader, and G. Graw, Nucl. Instrum. Methods Phys. Res. A **310**, 706 (1991).
- [26] R. Hertenberger, Ph.D. thesis, LMU, Munich, 1991.
- [27] B.D. Valnion, Ph.D. thesis, LMU, ISBN 3-89675-328-2, Munich, 1998.
- [28] F. Riess, fit program GASPAN, 1997 (unpublished).
- [29] W.T. Wagner, G.M. Crawley, G.R. Hammerstein, and H. McManus, Phys. Rev. C **3**, 757 (1975).
- [30] G.R. Satchler, *Direct Nuclear Reactions* (Oxford University Press, London, 1983).
- [31] G.R. Satchler, J. Math. Phys. **13**, 1118 (1972).
- [32] D. Hofer, M. Bisenberger, R. Hertenberger, H. Kader, H.J. Maier, E. Müller-Zanotti, P. Schiemenz, G. Graw, P. Maier-Komor, G. Molnár, W. Unkelbach, J. Hebenstreit, H. Ohm, D. Paul, P. von Rossen, and M. Fujiwara, Nucl. Phys. **A551**, 173 (1993).
- [33] T. Tamura, Rev. Mod. Phys. **37**, 371 (1965).
- [34] U. Atzrott, Ph.D. thesis, Universität Tübingen, Tübingen, 1995.
- [35] P. Schnitter, BL, LMU, and TUM, Garching, 1998 (private communication).
- [36] P. Schiemenz, Annual Reports, BL, LMU, and TUM, Garching, 1982–1984.
- [37] P.D. Kunz, Computer code DWUCK4, 1982 (unpublished).
- [38] F.D. Becchetti and G.W. Greenlees, Phys. Rev. **182**, 1190 (1969).
- [39] G. Perrin, Nguyen Van Sen, J. Arvieux, R. Darves-Blanc, J.L. Durand, A. Fiore, J.C. Gondrand, F. Merchez, and C. Perrin, Nucl. Phys. **A282**, 221 (1977).
- [40] W.W. Daehnick, J.D. Childs, and Z. Vrcelj, Phys. Rev. C **21**, 2253 (1980).
- [41] V.Yu. Ponomarev and P. von Neumann-Cosel, Phys. Rev. Lett. **82**, 501 (1999).
- [42] E-mail: vlad@thsun1.jinr.ru
- [43] F.J. Eckle, G. Eckle, F. Merz, H.J. Maier, H. Kader, and G. Graw, Nucl. Phys. **A501**, 413 (1989).
- [44] E.K. Warburton and B.A. Brown, Phys. Rev. C **43**, 602 (1991).
- [45] P. Grabmayr, G. Mairle, U. Schmidt-Rohr, G.P.A. Berg, J. Meissburger, P. von Rossen, and J.L. Tain, Nucl. Phys. **A469**, 285 (1987).
- [46] M.A.J. Mariscotti, D.R. Bes, S.L. Reich, H.M. Sofia, P. Hungerford, S.A. Kerr, K. Schreckenbach, D.D. Warner, W.F. Davidson, and W. Gelletly, Nucl. Phys. **A407**, 98 (1983).
- [47] J. Raynal, computer code ECIS, 1979 (unpublished).
- [48] S.A. Fayans, A.P. Platonov, G. Graw, and D. Hofer, Nucl. Phys. **A577**, 557 (1994).